Interference between reaction mechanisms in $^{32}S(^3He,n)^{34}Ar$

R. E. Benenson
Department of Physics, State University of New York, Albany, New York 12222

M. T. McEllistrem and J. L. Weil
Department of Physics and Astronomy, University of Kentucky, Lexington, Kentucky 40506

W. R. Coker and T. Tamura
Department of Physics, University of Texas, Austin, Texas 78712

(Received 27 June 1983)

Excitation curves for the $^{32}S(^3He,n_0)^{34}Ar$ reaction at selected angles, and n_0 and n_1 angular distributions at four energies below the Coulomb barrier were measured. The data were analyzed by considering the interference between direct-reaction and compound-nucleus formation amplitudes.

The measurements of the $^{32}S(^3He,n)^{34}Ar$ reaction presented here were stimulated by a previous observation concerning this reaction owing to McMurray *et al.*, an $L=0$ transition with an angular distribution which was strongly backward peaked.[1] A similarly anomalous angular distribution for the $^{20}Ne(^3He,n)^{22}Mg$ reaction had been observed and angular distributions at three energies were successfully interpreted by some of the present authors as owing to the interference between direct reaction (DR) and compound nucleus (CN) formation amplitudes.[2] In the latter work, we assumed a superposition of two resonances. Evidence for one appeared in the same experiment; the existence of the second was confirmed in a later experiment by Bose *et al.*[3]

In the present paper we report data on $^{32}S(He,n)^{34}Ar$ and analysis of the n_0 group based on the DR+CN interference hypothesis.[2] At $E(^3He)$ of about 6 MeV, the compound nucleus ^{35}Ar forms with an excitation energy $E_x \approx 18$ MeV, an energy and mass region in which fluctuation can become significant. Fluctuations are known to give rise to strongly energy-dependent cross sections and to pseudoresonances.[4–7] Our purpose was to learn if two-proton capture for this heavier mass region could again be interpreted as preferentially exciting resonance strength of definite spin and parity.

The plan was to locate resonance positions in advance of the interference analysis by means of excitation curves. The data sets were the following: (1) excitation curves for $^{32}S(^3He,n_0)^{34}Ar$ with $E(^3He)=4.6$–6.3 MeV at both 137.5° and 150° using an estimated 240 keV thick CdS target; (2) an excitation curve at 51° with $E(^3He)=4.6$–6.4 MeV using a 120 keV thick ZnS target, the latter also being used to repeat selected $E(^3He)$ regions at 137.5°; (3) $^{32}S(^3He,n_0)^{34}Ar$ and $^{32}S(^3He,n_1)^{34}Ar$ angular distributions at 5.0, 6.05, 6.4, and 6.5 MeV using the 120 keV thick target; and (4) elastic scattering $^{32}S(^3He,^3He)^{32}S$ measurements for $E(^3He)=4.75$–5.1 and 5.5–6.1 MeV using a ZnS target less than 20 keV thick, and with detectors placed at 30°, 84.5°, 121°, and 167°. The goal of locating resonance positions with data sets 1, 2, and 4 was only partially achieved.

The neutron angular distributions and excitation curves were measured with the University of Kentucky neutron time-of-flight facility which has an external bunching magnet. The system has been described previously.[8,9] Flight paths of 2.5 and 3.5 m, respectively, were used at backward and forward angles with pulsed beams of approximately 2 ns duration, and average beam currents of 1 to 2 μA. Targets were made by evaporating natural CdS or ZnS on tantalum backings. A 12.5 cm diam. by 5 cm thick liquid scintillator with n-γ discrimination was calibrated for efficiency vs E_n as described in Ref. 9. The neutron spectra were generally similar to that shown in Ref. 1, except that the $^{12}C(^3He,n_0)^{14}O$ peak was comparable to the n_1 and n_2 groups at forward angles and could not be fully resolved from the n_1 group. Carbon was always present despite the use of targets with a variety of different backings and the use of an in-line liquid nitrogen trap. Background measurements were performed by inserting a blank backing in front of the target, and the $^{12}C(^3He,n_0)^{14}O$ peak shape was subtracted where necessary from the $^{32}S(^3He,n_1)^{34}S$ spectrum peak. Target thicknesses were determined by switching to a deuteron beam and comparing yields from $^{32}S(d,n)^{33}Cl$ with the values published by Elbakr *et al.*[10]

Figure 1(a) shows an excitation curve at 137.5° measured with the 240 keV thick CdS target; data taken using the 120 keV target in selected energy regions are also shown. Similar data were obtained at 150°, and the backward peaking at $E(^3He)=5.6$ MeV, reported in Ref. 1, was confirmed. Figure 1(b) shows the excitation curve at 51°, where $P_2(\cos\theta)_{c.m.} \approx 0$; this angle was chosen with the expectation that the data would be an aid to the analysis.

The four energies shown by arrows in Fig. 1(b) were chosen for the angular distribution measurements: The three lower energies were expected to emphasize the interference effect, and the fourth at $E(^3He)_{lab}=6.50$ MeV was the highest energy available. A scattering chamber containing four solid state detectors was set up on a separate beam line for the elastic scattering measurements.

A salient feature of all $^{32}S(^3He,n_0)^{34}Ar$ excitation curves, including some not shown, is an isolated resonance

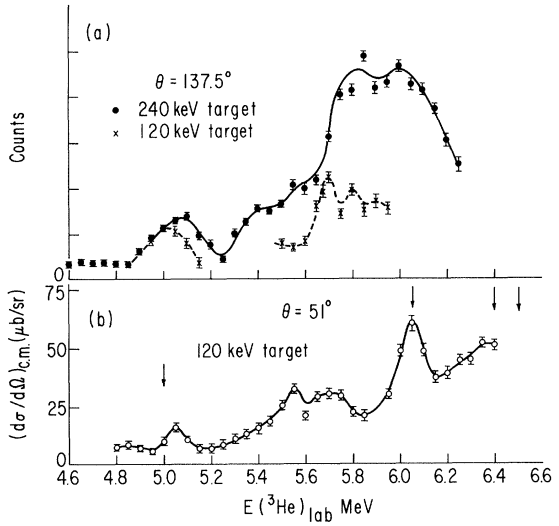

FIG. 1. Excitation curves for $^{32}S(^3He,n_0)^{35}Ar$. Target thicknesses are indicated. Arrows in part 1(b) show energies at which angular distributions were measured.

at $E(^3He)_{lab}=5.0$ MeV (which is not seen in the n_1 group). The 51° data in Fig. 1(b) also indicate a resonance at $E(^3He)_{lab}=6.05$ MeV. Both the 137.5° and 150° excitation curves suggest a doublet centered at approximately 5.7 MeV. What remains uncertain is whether the 6.05 MeV resonance is the upper member of the doublet, or if a still more complicated resonance structure exists in this energy region.

The elastic scattering data did not contribute any additional guidance in selecting resonance energies for the analysis. Small and uncertain deviations from a smooth energy dependence did not correspond in energy to the Fig. 1 anomalies. Almost unstructured elastic scattering excitation functions had also been previously encountered in the $^{20}Ne+^3He$ experiment, leading to the suggestion that the $(^3He,n_0)$ reaction channel is very weak, or that the resonances are the result of a final-state interaction. The absolute cross sections were <100 μb/sr.

Angular distributions for the n_0 and n_1 groups are shown, respectively, in Figs. 2 and 3. The strongest backward peaking in the present work occurs at the 5.0 MeV resonance. Above this energy angular distributions show rapid fluctuations in shape, asymmetry about 90°, and a central maximum. The estimated error in the scale factor for Figs. 2 and 3 is 30 percent. The highest attainable energy of 6.5 MeV is still below the $^3He+^{32}S$ Coulomb barrier; however, there is already considerable forward peaking, suggesting that the DR mechanism has become dominant.

The n_1 group angular distributions do not exhibit the characteristic DR $L=2$ shapes required by the $J=2^+$ assignment to the 2.09 MeV level,[11] a situation similar to what was found for $^{20}Ne(^3He,n_1)^{22}Mg$. In our theoretical analysis of the $^{32}S(^3He,n_0)$ angular distributions for $E(^3He)=5.0$, 6.05, 6.4, and 6.5 MeV, we assumed, as in Ref. 2, interference between compound-nucleus formation and a direct, two-proton transfer process. The direct process was described in terms of the distorted-wave Born ap-

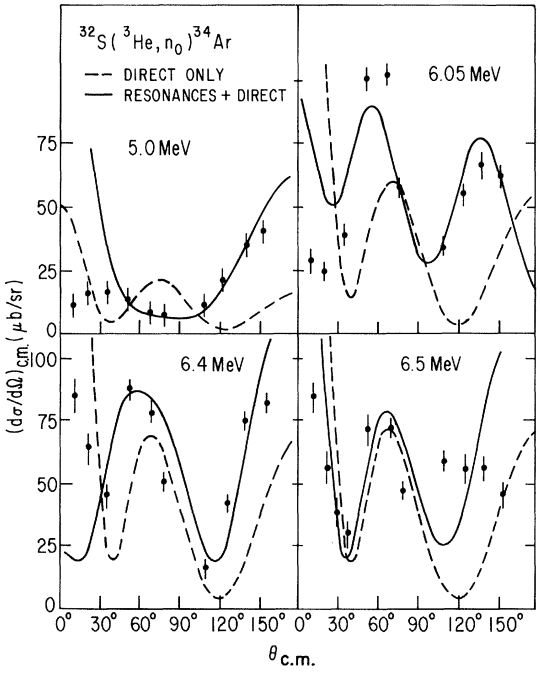

FIG. 2. Angular distributions of the neutron group for the $^{32}S(^3He,n_0)^{34}Ar$ reaction. Curves are labeled by $E(^3He)$ (lab). The dashed curves are DWBA calculations and the solid curves are obtained from the interference analysis discussed in the text. Error bars represent counting statistics only.

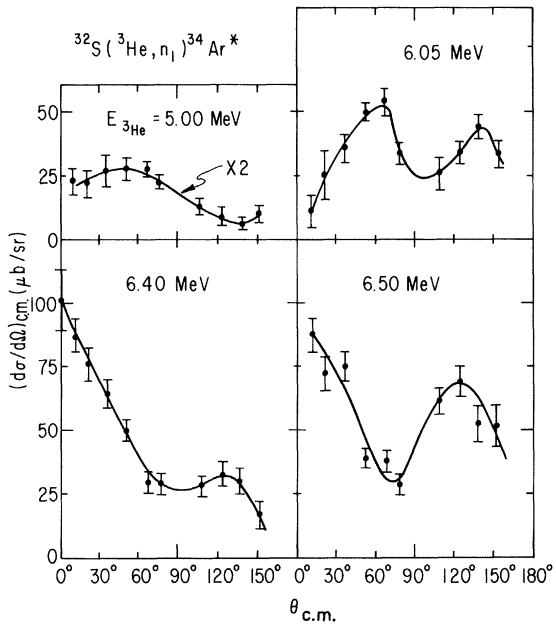

FIG. 3. Angular distributions for $^{32}S(^3He,n)^{34}Ar$. Solid lines are intended only to guide the eye. Error bars include the effect of subtracting the incompletely resolved $^{23}C(^3He,n_0)^{14}O$ contribution.

TABLE I. Optical parameters.

	V_0 (MeV)	W (MeV)	W_D (MeV)	V_{so} (MeV)	r (fm)	a (fm)	r' (fm)	a' (fm)	r_{so} (fm)	a_{so} (fm)	r_C (fm)
^{3}He	184.5	13.7	0.0	0.0	1.14	0.73	1.64	0.76	1.14	0.73	1.4
n	47.2	0.0	8.25	8.0	1.23	0.74	1.14	0.48	1.25	0.74	0.0
Bound state	113.6				1.25	0.65					

proximation (DWBA). Denoting the reaction process as $A(a,b)B$, the relevant amplitude is thus written as

$$A_{m_b m_a}(\theta)=A^{\mathrm{DWBA}}_{m_b m_a}(\theta)+A^{R}_{m_b m_a}(\theta)\ . \tag{1}$$

We consider only the transition from the 0^+ ground state of ^{32}S to the 0^+ ground state of ^{34}Ar; the resonance amplitude simplifies to[2,12]

$$A^{R}_{m_b m_a}(\theta)=-(\sqrt{\pi}/k_a)\sum_{\nu} e^{i(\delta_{j_a\nu}+\delta_{j_b\nu})}[\Gamma^{1/2}_{b\nu}\Gamma^{1/2}_{a\nu}/(E-E_\nu+i\Gamma_\nu/2)]$$
$$\times\hat{l}_a Y_{l_b,m_a-m_b}(\theta,0)\langle l_a 0 s_a m_a \mid J_\nu m_a\rangle\langle l_b m_a-m_b,s_b m_b \mid J_\nu m_a\rangle\ . \tag{2}$$

Here J_ν is the total angular momentum of the resonance ν, and the definite parity π_ν of the resonance fixes $l_a=l_b$ by $(-1)^{l_a}=(-1)^{l_b}=\pi_\nu$; also, $j_a=j_b=J_\nu$. We take the resonance phases $\delta_{j_a\nu}$ and $\delta_{j_b\nu}$ to be identical to the total phase shift (Coulomb plus nuclear) predicted by the optical model in channels $j_a l_a$ and $j_b l_b$, respectively. To equate the resonance phases and the optical model phase shifts is justified in the shell-model theory of reactions.[13,14]

In computing these amplitudes the choice of parameters is not a simple matter. The optical model parameters for ^{3}He and n at these low energies are not very well known; see, for instance, Perey and Perey.[15] For each resonance we have five parameters to specify, J_ν, π_ν, E_ν, Γ_ν, and $g=\Gamma^{1/2}_{b\nu}\Gamma^{1/2}_{a\nu}$, and it is unclear how many resonances need to be considered for each energy region. We have therefore used the excitation function data (Fig. 1) to limit somewhat artificially the number of resonances considered. Beginning with only the two clear resonances at 5.0 and 6.05 MeV (4.6 and 5.6 MeV, c.m.), we have added as few other resonances as possible, two others to be specific, to search for sets of parameters which will reproduce the trends of the experimental angular distributions.

The procedure adopted was as follows: For each angular distribution, at 5.0, 6.05, 6.4, and 6.5 MeV, respectively, the fit was optimized using the direct contribution and a single (the nearest) resonance only. Then the other three resonances were added and the fit reoptimized. Various sets of optical parameters were tried; the results shown were obtained with potentials[15] shown in Table I, where the notation is standard. The diproton transferred was treated as an $L=J=0$, $N=3$ cluster bound by 6.95 MeV in ^{34}Ar (see Table I for the potential parameters). The nonmicroscopic form factor is completely adequate because only the tail of the form factor contributes to the DWBA amplitudes below the Coulomb barrier. Pure DWBA cross sections, calculated using program VENUS,[16] are shown by the dashed curves in Fig. 2. The two-proton, transition dependent structure factor ND_0^2 appearing in the DWBA amplitude was kept fixed for all calculations at the value given in Table II.

The parameters given in Table II, and the resulting fits, shown as solid curves in Fig. 2, were chosen as the most satisfactory compromise subject to our constraints: (a) a maximum of four resonances, (b) general agreement with absolute cross sections at all four energies, (c) use only of previously published optical parameters, and (d) enhancement of back angle cross sections. After the analysis was first completed, it was rerun fixing the third resonance at 5.2 MeV (c.m.) as suggested by the thinner target data of Fig. 1(a) and the unresolved doublet, but no significant improvement or other change resulted. No differing spin assignments for the first three resonances of Table II gave predictions bearing any resemblance to the data. The forward-angle behavior of the 6.05 and 6.4 MeV predictions appears to be permuted, the 6.4 MeV interference best fitting the 6.05 MeV data and vice versa. These conclusions are deceptive; interchanging the $\frac{3}{2}^+$ and $\frac{5}{2}^+$ assignments destroys the fit totally at intermediate and backward angles while leaving the forward angle predictions unchanged. We feel, therefore, that the spin assignments in Table II for the first three resonances are fairly firm. However, the J and position of the fourth resonance are not to be taken as seriously. It presumably is just a stand-in for a number of resonances affecting the 6.5 MeV angular distribution in various, relatively weak ways. Only in isolation does it give a fair fit to the 6.5 MeV an-

TABLE II. Parameters obtained in the analysis of the angular distributions of Fig. 2.

J^π	E_ν (MeV)	Γ_ν (MeV)	$\Gamma^{1/2}_{^3\mathrm{He}}\Gamma^{1/2}_{\mathrm{n}}$	$ND_0^2\times10^4$ (MeV^2 fm^3)
$\frac{1}{2}^+$	4.540	0.050	0.00367	0.204
$\frac{3}{2}^+$	5.465	0.070	0.00650	0.204
$\frac{5}{2}^+$	5.835	0.070	0.00558	0.204
$\frac{1}{2}^+$	5.9535	0.030	0.00354	0.204

gular distribution, and this does not improve by an alternative choice of resonance energy.

When we adjust the resonance parameters to optimize the fit, only intermediate and backward angles show reasonable agreement with the data. The character of the forward-angle interference for a given set of resonance parameters is mainly sensitive to the phase of the corresponding DWBA amplitude, and thus mainly to the set of optical parameters chosen. However, no potentials were found in the tabulations[14,16] which would give precisely the character of the forward angle interference observed at all four energies considered; in view of the difficulty in describing the neutron channel in terms of an optical potential at these energies, this situation is hardly surprising.

Shotter *et al.*[4] have shown that fluctuations can be significant for $\langle\Gamma\rangle/D\approx 1$, where $\langle\Gamma\rangle$ is the average level width and D the level density. This ratio can only be estimated for $E_x\approx 18$ MeV in ^{35}A, since the Endt-van der Leun tabulation[11] stops at 8 MeV and shows there only about six levels/MeV with no apparent trend toward increase. Based on results[5,18] from neighboring nuclei, $10\lesssim\langle\Gamma\rangle\lesssim 30$ keV; D can be estimated from Gilbert and Cameron's formula[19] as 3 and 2 keV, respectively, for $J=\frac{1}{2}$ and $\frac{3}{2}$. Assuming the latter values as lower limits and taking the upper limit of D at the 8 MeV value, the ratio appears to lie between about 0.1 and 10. We therefore cannot rule out some contribution by fluctuations to the excitation curves and angular distributions.

Nevertheless, we continue to believe that the concept of trying to describe the data by considering interference between DR and CN processes is essentially correct. We base this on the improvement of back-angle fits over DR alone, reasonable absolute differential cross sections over our entire range, and the inflexibility of the spin assignments. The fits are certainly less satisfactory than in the simpler ^{20}Ne(^{3}He,n)^{22}Mg case. The results may be interpreted as indicating enhancements of s and d strength in a region of fairly closely spaced levels, most of which are not strongly excited by two-proton transfer; our isolated-resonance analysis would thus remain valid despite $\langle\Gamma\rangle/D$ being of order 1. Futhermore, for $E(^3\text{He})>5.6$ MeV (see also Ref. 1) each angular distribution shows a well-defined central maximum in agreement with DWBA predictions rather than the more random energy variation associated with fluctuations; and by $E(^3\text{He})=6.5$ MeV the DR mechanism appears to dominate.

One of us (R.E.B.) gratefully acknowledges the hospitality shown him by Dr. McEllistrem and the personnel at the University of Kentucky facility. We also sincerely thank Dr. D. F. Coope and Dr. S. N. Tripathi for considerable assistance in taking data. The research was supported by the National Science Foundation and the Research Foundation of the State of New York (R.E.B.), the National Science Foundation (M.T.M. and J.L.W.), and the U. S. Department of Energy (W.R.C and T.T.).

[1]W. R. McMurray, P. Van der Merwe, and I. J. Van Heerden, Nucl. Phys. A92, 401 (1967).
[2]R. E. Benenson, I. J. Taylor, D. L. Bernard, H. H. Wolter, and T. Tamura, Nucl. Phys. A197, 305 (1972).
[3]S. K. Bose, A. Kogan, and P. R. Bevington, Nucl. Phys. A219, 115 (1974).
[4]A. C. Shotter, P. S. Fisher, and D. K. Scott, Nucl. Phys. A159, 577 (1970).
[5]T. Ericson and T. Mayer-Kuckuk, Annu. Rev. Nucl. Sci. 16, 183 (1966).
[6]W. von Witsch, P. von Brentano, T. Mayer-Kuckuk, and A. Richter, Nucl. Phys. 80, 394 (1966).
[7]E. Almqvist, D. A. Bromley, J. A. Kuehner, and B. Whalen, Phys. Rev. 130, 1140 (1963).
[8]F. D. McDaniel, J. D. Brandenberger, G. P. Glasgow, and H. G. Leighton, Phys. Rev. C 10, 1087 (1974).
[9]D. F. Coope, S. N. Tripathi, M. C. Schell, J. L. Weil, and M. T. McEllistrem, Phys. Rev. C 16, 2223 (1977).
[10]S. A. Elbakr, C. Glavina, W. K. Dawson, V. K. Gupta, W. J. McDonald, and G. C. Neilson, Can. J. Phys. 50, 674 (1972).
[11]P. M. Endt and C. Van der Leun, Nucl. Phys. A310, 1 (1978).
[12]A. M. Lane and R. G. Thomas, Rev. Mod. Phys. 30, 257 (1958).
[13]U. Fano, Phys. Rev. 124, 1866 (1961).
[14]C. Mahaux and H. A. Widenmüller, *Shell-Model Approach to Nuclear Reactions* (North-Holland, Amsterdam, 1969), Chap. 3.
[15]C. M. Perey and F. G. Perey, At. Data Nucl. Data Tables 17, 1 (1976).
[16]T. Tamura, W. R. Coker, and F. Rybicki, Comput. Phys. Commun. 2, 94 (1971).
[17]A. E. S. Green, T. Sawada, and D. S. Saxon, *The Nuclear Independent Particle Model* (Academic, New York, 1968), p. 226.
[18]D. Shapira, R. G. Stokstad, and D. A. Bromley, Phys. Rev. C 10, 1063 (1974).
[19]A. Gilbert and A. G. W. Cameron, Can. J. Phys. 43, 1446 (1965).